CHEMISTRY OF MATERIALS

Article

pubs.acs.org/cm

Structure and Properties of Polymer Electrolyte Membranes Containing Phosphonic Acids for Anhydrous Fuel Cells

Sung-Il Lee,[†] Kyung-Hwan Yoon,[†] Myeongsoo Song,[†] Huagen Peng,[‡] Kirt A. Page,*[,‡] Christopher L. Soles,[‡] and Do Y. Yoon*[,†]

[†]Department of Chemistry, Seoul National University, Seoul 151-747, Korea

[‡]Polymers Division, National Institute of Standards and Technology, Gaithersburg, Maryland 20899, United States

Supporting Information

ABSTRACT: Recently, water-free, proton-conducting polymer electrolytes have been attracting attention because of their possible application as fuel cell membranes at intermediate temperatures (100 to 200 °C). Phosphonic acid groups are considered feasible anhydrous proton conducting moieties due to the high degree of proton self-dissociation arising from their intrinsic amphoteric character and high mobility of protonic charge carriers. In this work, we have synthesized and characterized model, phosphonic acid-functionalized proton-conducting polymers, poly(vinylbenzyloxy-alkyl-phosphonic acid)s, for the purpose of exploring the relationship between molecular design, nanostructure, and performance characteristics. These novel proton conducting materials were characterized for their thermal stability, nanostructure, and performance properties. Thermogravimetric analysis (TGA) indicates that the polymers are thermally stable up to 140 °C, where the condensation of phosphonic acid groups starts to occur. Results from small-angle X-ray scattering (SAXS) show a peak corresponding to a Bragg spacing of approximately 21−24 Å, which is attributed to layerlike structure formation of the phosphonic acid containing conducting channels. The proton conductivity increases with temperature, reaching a value on the order of 3×10^{-4} S/cm at 140 °C under nominally anhydrous conditions.

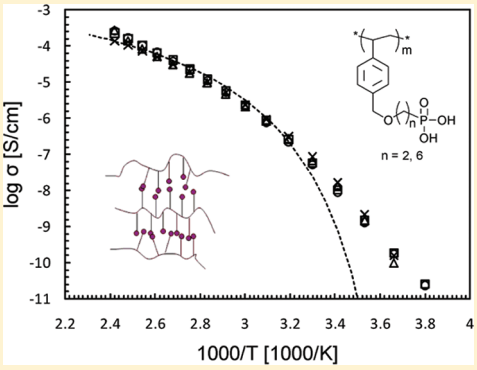

KEYWORDS: *polymer electrolyte membrane, anhydrous fuel cell, phosphonic acid*

INTRODUCTION

In recent years, polymer electrolyte (or proton exchange) membrane fuel cells (PEMFCs) have been considered as a promising energy conversion system for applications ranging from small-scale power sources for portable electronic devices to automotive power supplies because of their high current densities, fast start capability, and the ability to construct compact, lightweight cells.[1,2] The polymer electrolyte membrane (PEM), which is one of the key components in a PEMFC, acts both as a separator to gas permeation from the anode to cathode as well as a solid electrolyte proton conductor. The most widely used PEM material has been the polyperfluorosulfonic acid (poly-PFSA), Nafion produced by DuPont, because of its excellent chemical and thermal stability as well as its high proton conductivity. The sulfonic acid groups facilitate proton conduction but require a minimal level of hydration to have considerable conductivity (e.g., $\sigma = 0.1$ S/cm, λ (moles of H_2O/mol of SO_3H) = 22).[3] However, these hydrated PEMs have significant shortcomings that begin to limit performance at operating temperatures near 100 °C, where the water content begins to drop, resulting in a significant decrease in the proton conductivity. As a result, operation temperature of the fuel cell is limited to a temperature somewhat below the boiling point of water (approximately 80 °C). Under such operating conditions one encounters serious problems such as carbon monoxide poisoning of the catalyst layer, complicated heat and water management, and water/methanol crossover.[4−6] The desired optimal PEM material would need to exhibit a conductivity of greater than 0.1 S/cm, with a water content on the order of 20% by volume at an operating temperature of 120 °C.[7]

One strategy to achieving these goals is to develop new proton conducting materials capable of operating under low humidity, or anhydrous conditions, and at intermediate temperatures (100 to 200 °C).[8−10] Phosphoric acid doped polybenzimidazole (PBI/H_3PO_4) blends have been studied extensively and exhibit relatively high proton conductivity (ca. 0.03 S/cm) at approximately 150 °C. The main disadvantage of these blends is that the H_3PO_4 small molecules, while in excess of the base sites, can diffuse out of the membrane over time.[11,12] A more recent approach is to attach heterocyclic molecules such as imidazole, benzimidazole, and pyrazole to oligomeric or polymeric systems via flexible spacers.[9,13−16] This is because heterocycles are ideal proton solvents and can be

Received: July 19, 2011
Revised: November 5, 2011
Published: November 9, 2011

substituted for water because of their amphoteric character and hydrogen bond formation similar to water molecules. In addition, the higher boiling point of heterocycles compared to water enables a PEM-based fuel cell to operate at higher temperature. For these heterocyclic proton conductors, it is more likely that proton transport is facilitated by structural diffusion of the protogenic groups, also known as the Grotthuss mechanism, under water-free condition.[17,18] Schuster et al.[19] compared the use of different protogenic groups at intermediate temperatures for low humidity PEMFCs including sulfonic acid groups, phosphonic acid groups and imidazole groups as model compounds. They concluded that, at intermediate temperatures (120 to 160 °C) and low humidity, the phosphonic acid group is the most suitable proton conductor. A high degree of self-dissociation, which results from more pronounced intrinsic amphoteric character of phosphonic acid, and a high mobility of the protonic charge carrier were two key factors that were thought to contribute to the observed higher proton conductivity. In addition, phosphonic acid has comparatively better electrochemical and thermo-oxidative stability and allows higher reaction rates for hydrogen oxidation and oxygen reduction on Pt electrode surfaces. These results reveal that phosphonic acid is very attractive as a protogenic group in anhydrous proton conducting polyelectrolytes. On the basis of such results, immobilized phosphonic acid based systems were prepared by tethering phosphonic acid groups to a polymer backbone. The simplest case of a polymer containing phosphonic acid found in the literature is poly(vinylphosphonic acid) (PVPA).[20] The proton conductivity of this material in the nominally dry state was determined to be on the order of 1×10^{-4} to 1×10^{-3} S/cm at approximately 150 °C. The proton conductivity is attributed to the formation of interconnected, mobile aggregates of phosphonic acid groups and the consequent Grotthus mechanism.[10] Additionally, copolymers of PVPA[21,22] and blends with heterocycles[23,24] were investigated along with acid−base composite materials[25,26] based on phosphate and imidazole. Despite its ability to conduct protons, PVPA has poor mechanical properties for use in a fuel cell in large part due to its low glass transition temperature ($T_g \approx -23$ °C).[23] To solve this problem, researchers have turned to incorporating aromatic groups into the polymer structure to improve the chemical and thermal stability of the PEM for practical applications.[27−31]

In this work, a pair of model polystyrene derivatives containing phosphonic acid side groups, with varying spacer lengths, were prepared by the Michealis−Arbuzov reaction and other synthetic methods. The polystyrene backbone was selected due to its facile polymerization and better mechanical properties including a significantly higher T_g as compared to PVPA. The incorporation of flexible spacers will allow sufficient mobility to the protogenic group to facilitate conductivity via charge motion. Moreover, the surfactant-like structure of the side chain would promote a micro or nano phase-separation of phosphonic acid aggregates,[32] which could serve as pathways for proton conduction while the polystyrene-like backbone provides the improved mechanical performance including a high T_g. The molecular masses, thermal stability, structure−property relationships, and proton conductivity of these anhydrous fuel cell membrane materials were studied employing a variety of experimental techniques including aqueous gel permeation chromatography (GPC), thermogravimetric analysis (TGA), small-angle X-ray scattering (SAXS), dynamic mechanical analysis (DMA), and broadband dielectric relaxation spectroscopy (DRS).

EXPERIMENTAL SECTION

Certain commercial equipment, instruments, or materials are identified in this paper in order to specify the experimental procedure adequately. Such identification is not intended to imply recommendation or endorsement by the National Institute of Standards and Technology, nor is it intended to imply that the materials or equipment identified are necessarily the best available for the purpose.

Materials. 4-vinylbenzyl chloride, ethylene glycol, tri(ethylene)-glycol, 1,6-hexanediol, sodium hydride, *p*-toluenesulfonyl chloride, triethylamine (TEA), sodium iodide, triisopropyl phosphite, N,N-dimethylformamide (DMF), acetone, 2,2′-azobis(isobutyramidine) dihydrochloride (AIBA), hydroquinone were purchased from Sigma-Aldrich, Inc. and bromotrimethylsilane from TCI Chemical Inc. All reagents mentioned above were used without any further purification. Dichloromethane, a reaction solvent, was distilled over calcium hydride (CaH_2). Spectra/Por dialysis membrane with molecular cutoff value of 2000 was purchased from Spectrum Laboratories, Inc.

Measurements. ^{1}H NMR and ^{13}C NMR spectra were obtained with a Bruker Fourier Transform DPX-300 MHz nuclear magnetic resonance spectrometer at room temperature in $CDCl_3$ and DMSO-d_6. Chemical shifts were measured in parts per million (δ value) from tetramethylsilane as an internal standard.

The relative molecular weights of polymers were determined against a poly(ethyleneglycol) standard calibration in an aqueous gel permeation chromatography (GPC) system, comprised of Waters 515 pump, PL aquagel OH 30 column (column temperature 35 °C) and Waters 2410 differential refractometer. A mixture of pH 9.0 buffer (70 vol %) and methanol (30 vol %) was eluted at a flow rate of 1.0 mL/min. Into the GPC, 100 μL of sample solution with a concentration of 3 mg/mL was injected.

Thermogravimetric analysis (TGA) was carried out with TGA Q50 (TA Instruments). The temperature was raised at a rate of 10 °C/min from 30 to 700 °C with a constant nitrogen gas purge rate of 60 mL/min. Glass transition temperatures were determined with a differential scanning calorimeter (DSC Q1000, TA Instruments) at a heating rate of 20 °C/min from −70 to 100 °C. Prior to measurements, samples were kept in a vacuum oven at 60 °C for 2 days to completely remove residual water or solvents.

Dynamic mechanical analysis (DMA) was carried out with DMA 2980 (TA Instruments), at a controlled force mode with a penetration clamp. The polymer samples were prepared in shape of pressed pellets (diameter, 12 mm) and dried out in a vacuum oven at 60 °C for 24 h. A flat probe penetrated into the pellet with a static force of 0.5 N at a heating rate of 1 °C/min from 20 to 120 °C.

Small-angle X-ray scattering (SAXS) measurements were performed on a laboratory X-ray scattering instrument that utilizes pinhole collimated CuK_α radiation, using three consecutive pinholes with diameters of 1000 μm, 400 μm, and 300 μm, decreasing in diameter as the incident beam approaches the sample. Two-dimensional scattering patterns from the fuel cell membrane were collected on an image plate detector under vacuum to reduce the scattering from the air. The sample-to-detector distance (SDD) is 21.3 cm, which provides a wave vector (Q) range from 1 to 20 nm^{-1}. Here, Q is expressed by the equation, $Q = (4\pi/\lambda)\sin\theta$, where λ is the wavelength of Cu$K\alpha$, 0.154 nm at 8.04 keV, and 2θ is the scattering angle.

Ionic conductivities were measured under dry nitrogen atmosphere using broadband dielectric spectrometer from NOVOCONTROL GmbH, Germany, in the temperature range from −10 to 140 °C, with temperature intervals of 10 °C over a frequency range from 10^{-2} Hz to 10^7 Hz. Temperature was controlled with the Novocontrol Quatro Cryosystem with a set point precision of 0.1 °C. The measurements were performed over several heating and cooling cycles to determine the stability and reproducibility of the results. All samples for conductivity measurements were obtained by preparing solvent-cast films and then drying them under vacuum at 60 to 70 °C for 3 days to remove residual solvents/water and to obtain the nominally dry

dx.doi.org/10.1021/cm202064x | *Chem. Mater.* 2012, 24, 115−122

sample as previously reported.[10] The films were sandwiched between two gold-plated electrodes (diameter, 10 mm, 35 mm) using a Teflon spacer (thickness, 129.5 μm).

Synthesis of Monomers. ***2-(4-Vinyl-benzyloxy)-ethanol (2a).*** Ethylene glycol (16.7 mL, 0.30 mol) was added dropwise to a stirred solution of sodium hydride (4.8 g, 0.12 mol, 60% dispersion in mineral oil) in N,N-dimethylformamide (DMF) (50 mL) at 0 °C. After the solution was stirred over 1 h, 4-vinylbenzyl chloride (**1**, 14.1 mL, 0.10 mol) was added dropwise to the suspension, using a syringe at 0 °C and vigorously stirred at room temperature. After 20 h of stirring, 300 mL of water was poured into the solution. Ethyl acetate was used to extract organic products (3 × 300 mL). The organic layer was collected and dried over anhydrous magnesium sulfate. The solvent was removed by a rotary evaporator. The product was further purified by a silica gel column chromatography. 11.0 g (62%) of **2a** was obtained as a colorless liquid. ^{1}H NMR (300 MHz, $CDCl_3$) δ 7.39 (d, 2H), 7.29 (d, 2H), 6.71 (dd, 1H), 5.74 (d, 1H), 5.24 (d, 1H), 4.53 (s, 2H), 3.73(t, 3H), 3.57 (t, 3H), 2.29 (s, 1H).

*Toluene-4-sulfonic Acid 2-(4-vinyl-benzyloxy)-ethyl Ester (**3a**).* *p*-Toluenesulfonyl chloride (22.9 g, 0.12 mol) was dissolved in distilled dichloromethane (80 mL) and **2a** (18.2 g, 0.10 mol) was added to the stirred solution dropwise at 0 °C. After stirring for 30 min, triethylamine (16.7 mL, 0.12 mol) was added dropwise and the solution was stirred at room temperature overnight. The product was extracted with water and diethyl ether (3 × 200 mL). The organic layer was collected and dried over anhydrous magnesium sulfate. The solvent was evaporated by a rotary evaporator. The product was further purified by a silica gel column chromatography. 11.0 g (33%) of **3a** was obtained as a colorless liquid. ^{1}H NMR (300 MHz, $CDCl_3$) δ 7.79 (d, 2H), 7.37 (d, 2H), 7.30 (d, 2H), 7.21 (d, 2H), 6.71 (dd, 1H), 5.74 (d, 1H), 5.24 (d, 1H), 4.46 (s, 2H), 4.19 (t, 2H), 3.65 (t, 2H), 2.43 (s, 3H).

*1-(2-Iodo-ethoxymethyl)-4-vinyl-benzene (**4a**).* Sodium iodide (27 g, 0.18 mol) was dissolved in 300 mL of anhydrous acetone. **3a** (30 g, 0.090 mol) was added dropwise and the mixture was heated to reflux for 15 h. Acetone was removed by a rotary evaporator and the mixture was extracted with water and diethyl ether (3 × 150 mL). The organic layer was collected and dried over anhydrous magnesium sulfate. The solvent was removed by a rotary evaporator. The product was further purified by a silica gel column chromatography. 18.8 g (91%) of **4a** was obtained as a yellowish liquid. ^{1}H NMR (300 MHz, $CDCl_3$) δ 7.40 (d, 2H), 7.31 (d, 2H), 6.71 (dd, 1H), 5.75 (d, 1H), 5.25 (d, 1H), 4.79 (s, 2H), 3.73(t, 2H), 3.27 (t, 2H).

*[2-(4-Vinyl–benzyloxy)-ethyl]-phosphonic Acid Diisopropyl Ester (**5a**).* Triisopropyl phosphite (3.8 mL, 0.017 mol), **4a** (5.3 g, 0.018 mol) and hydroquinone (0.0594 g, 0.53 mmol) was mixed in a round-bottomed flask without solvent. The reaction temperature was first raised to 90 °C with vigorous stirring and gradually increased to 120 °C. The reaction mixture was stirred for 14 h at 120 °C, then was loaded directly on the top of a silica gel column chromatography for purification. 4.4 g (81%) of **5a** was obtained as a colorless liquid. ^{1}H NMR (300 MHz, $CDCl_3$) δ 7.38 (d, 2H), 7.29 (d, 2H), 6.71 (dd, 1H), 5.76 (d, 1H), 5.23 (d, 2H), 4.69 (m, 2H), 4.50 (s, 2H), 3.72 (m, 2H), 2.12 (td, 2H), 1.29 (s, 12H); ^{13}C NMR (300 MHz, $CDCl_3$) δ 137.6, 137.2, 136.6, 128.0, 126.3, 114.0, 72.8, 64.3, 61.8, 61.7, 28.1, 26.2, 16.6 (× 2), 16.5 (× 2).

*[2-(4-Vinyl-benzyloxy)-ethyl]-phosphonic Acid (**6a**).* A dried round-bottomed flask was filled with 5 mL of distilled dichloromethane and **5a** (3.4 g, 0.010 mol) was added with stirring. Bromotrimethylsilane (3.0 mL, 0.023 mol) was added dropwise for 10 min under nitrogen gas flow. After the color of the solution was changed from colorless to yellowish, the mixture was stirred for 5 h at the room temperature. Most of the solvent and unreacted bromotrimethylsilane was removed by a rotary evaporator and a subsequent high vacuum-dry. Five milliliters of deionized water was added and the mixture was stirred for 3 h. The water and residual solvent were removed by a rotary evaporator and the product was completely dried in a high vacuum. **6a** (2.3 g, 95%) was yielded as a yellowish solid. ^{1}H NMR (300 MHz, $CDCl_3$) δ 8.80 (s, 2H), 7.32 (d, 2H), 7.22 (d, 2H), 6.65 (dd, 1H), 5.69 (d, 2H), 5.20 (d, 2H), 4.42 (s, 2H), 3.71 (m, 2H), 2.13 (td, 2H); ^{13}C NMR (300 MHz, $CDCl_3$) δ 137.3, 137.0, 136.6, 128.2, 126.4, 114.1, 72.6, 64.2, 28.2, 26.4.

*2-(4-Vinyl-benzyloxy)- hexan-1-ol (**2b**).* To a stirred solution of 1, 6-hexandiol (35.4 g, 0.30 mol) in DMF (55 mL) was slowly added sodium hydride (4.8 g, 0.12 mol, 60% dispersion in mineral oil) at 0 °C. After the solution was stirred over 1 h, 4-vinylbenzyl chloride (**1**, 14.1 mL, 0.10 mol) was added dropwise using a syringe at 0 °C and vigorously stirred for 20 h at the room temperature. The same workup and purification procedure described for **2a** was carried out and 18.1 g (77%) of **2b** was obtained as a colorless liquid. ^{1}H NMR (300 MHz, $CDCl_3$) δ 7.39 (d, 2H), 7.29 (d, 2H), 6.71 (dd, 1H), 5.74 (d, 1H), 5.23 (d, 1H), 4.48 (s, 2H), 3.62 (t, 2H), 3.46 (t, 2H), 1.68−1.51 (m, 4H), 1.49 (s, 1H), 1.45−1.30 (m, 4H).

*Toluene-4-sulfonic Acid 6-(4-Vinyl-benzyloxy)-hexyl Ester (**3b**).* *p*-Toluenesulfonyl chloride (38.6 g, 0.20 mol) was dissolved in distilled dichloromethane (120 mL) and cooled to 0 °C. **2b** (36.0 g, 0.15 mol) was added to the stirred solution dropwise at 0 °C. After stirring for 30 min, triethylamine (27.6 mL, 0.20 mol) was added dropwise. The solution was stirred overnight at the room temperature. The same workup and purification procedure described for **3a** was applied and 57.2 g (95%) of **3b** was obtained as a colorless liquid. ^{1}H NMR (300 MHz, $CDCl_3$) δ 7.78 (d, 2H), 7.38 (d, 2H), 7.32 (d, 2H), 7.27 (d, 2H), 6.71 (dd, 1H), 5.74 (d, 1H), 5.23 (d, 1H), 4.46 (s, 2H), 4.01 (t, 2H), 3.41 (t, 2H), 2.43 (s, 3H), 1.69−1.49 (m, 4H), 1.38−1.24 (m, 4H).

*1-(6-Iodo-hexoxymethyl)-4-vinyl-benzene (**4b**).* Sodium iodide (49.5 g, 0.33 mol) was dissolved in 300 mL of anhydrous acetone. **3b** (57.0 g, 0.15 mol) was added dropwise and the solution was refluxed for 40 h. Acetone was removed by a rotary evaporator and the mixture was extracted with water and diethyl ether (3 × 150 mL). The same workup and purification procedure described for **4a** was applied to obtain 41.5 g (82%) of **4b** as a yellowish liquid. ^{1}H NMR (300 MHz, $CDCl_3$) δ 7.39 (d, 2H), 7.29 (d, 2H), 6.71 (dd, 1H), 5.74 (d, 1H), 5.23 (d, 1H), 4.48 (s, 2H), 3.45 (t, 2H), 3.18 (t, 2H), 1.88−1.76 (m, 2H), 1.68−1.55 (m, 2H), 1.46−1.33 (m, 4H).

*[6-(4-Vinyl-benzyloxy)-hexyl]-phosphonic Acid Diisopropyl Ester (**5b**).* In a round-bottomed flask, **4b** (5.2 g, 0.015 mol), triisopropyl phosphite (3.1 mL, 0.014 mol) and hydroquinone (0.0495 g, 0.45 mmol) were mixed. The reaction temperature was first raised to 90 °C with vigorous stirring and gradually increased to 120 °C. The reaction mixture was stirred for 14 h and then loaded directly on the top of a silica gel column chromatography for purification. 3.7 g (71%) of **5b** was obtained as a colorless liquid. ^{1}H NMR (300 MHz, $CDCl_3$) δ 7.39 (d, 2H), 7.29 (d, 2H), 6.71 (dd, 1H), 5.74 (d, 1H), 5.23 (d, 1H), 4.68 (m, 2H), 4.48 (s, 2H), 3.45 (t, 2H), 1.74−1.50 (m, 6H), 1.44−1.35 (m, 4H), 1.30 (d, 12H); ^{13}C NMR (300 MHz, $CDCl_3$) δ 138.3, 137.0, 136.7, 127.9, 126.3, 113.8, 72.7, 70.3, 61.5, 61.4, 30.6, 30.4, 29.6, 26.7, 25.8, 24.8, 22.5, 22.4, 16.6 (× 2), 16.5 (× 2).

*[6-(4-Vinyl-benzyloxy)-hexyl]-phosphonic Acid (**6b**).* A dried round-bottomed flask was filled with 5 mL of distilled dichloromethane and **5b** (3.1 g, 0.0081 mol) was added with stirring. After achieving a homogeneous solution, bromotrimethylsilane (2.4 mL, 0.018 mol) was added dropwise for 10 min under nitrogen gas flow. After the color of the solution was changed from colorless to yellowish, the mixture was stirred for 5 h at room temperature. The same workup and purification procedure described in **6a** was applied to obtain **6b** (2.2 g, 93%) as a yellowish solid. ^{1}H NMR (300 MHz, $CDCl_3$) δ 9.51 (s, 2H), 7.36 (d, 2H), 7.26 (d, 2H), 6.68 (dd, 1H), 5.72 (d, 1H), 5.21 (d, 1H), 4.46 (s, 2H), 3.42 (t, 2H), 1.81−1.49 (m, 6H), 1.42−1.26 (m, 4H); ^{13}C NMR (300 MHz, $CDCl_3$) δ 138.0, 137.1, 136.7, 128.1, 126.4, 113.9, 72.7, 70.4, 30.4, 30.2, 29.5, 26.9, 25.7, 25.0, 22.2, 22.1.

Polymerization. Monomer **6a** (1.31 g, 0.0054 mol) and 2,2′-azobis(isobutyramidine) dihydrochloride (AIBA) (0.015 g, 0.054 mmol, 1 mol-%) were put together in a Schlenk tube and dissolved in 6 mL (1 mol/L) of 1,4-dioxane/deionized water (v/v = 3/2). The solution was degassed by freeze−pump−thaw procedures: the reaction mixture was completely frozen in liquid nitrogen for 4 min, the tube was evacuated for 1 min, and warmed to the room temperature. The whole procedure was repeated over 3 times. The Schlenk tube was charged with nitrogen gas and the solution was stirred at 70 °C for 14

dx.doi.org/10.1021/cm202064x | *Chem. Mater.* 2012, 24, 115−122

Scheme 1. Synthesis of Styrene-Derivative Monomers Containing the Phosphonic Acid

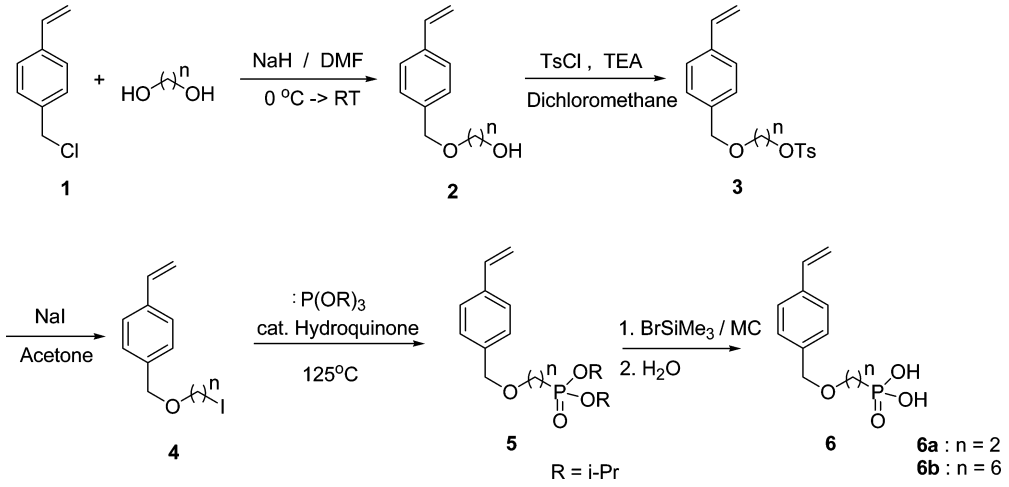

Scheme 2. Polymerization of Styrene-Derivative Monomers Containing the Phosphonic Acid

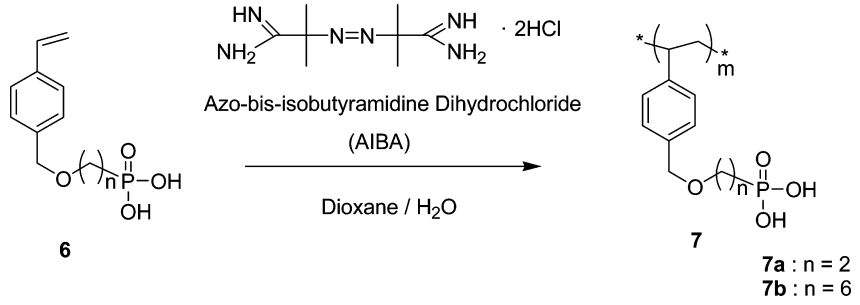

h. The resulting product was diluted with a small amount of deionized water and poured into a Spectra/Por dialysis membrane with a molecular cutoff value of 2000. After the polymer was purified by a dialysis method for 5 days, water and residual solvent were removed by freeze-drying. Polymer **7a** (denoted as PVBPA-Ethyl) was obtained as a yellowish-white powder (0.86 g, 66%). Monomer **6b** (1.28 g, 0.0043 mol) and AIBA (0.012 g, 0.043 mmol) were put together in a Schlenk tube and dissolved in 6 mL of 1,4-dioxane/deionized water (v/v = 3/2). The polymerization was performed by the same procedure as described above. Polymer **7b** (denoted as PVBPA-Hexyl) was obtained as a yellowish-white powder (0.81 g, 63%).

RESULTS AND DISCUSSION

Synthesis of Monomers and Polymerization. Styrene derivatives with phosphonic acid were prepared as described in Scheme 1. Two alkyl chains with different numbers of carbon units (ethyl and hexyl) were attached onto the styrene aromatic ring by a simple substitution reaction of the diol compound and 4-vinylbenzyl chloride as the starting reagent using NaH. To increase the yield of the monosubstituted diol compound in the first reaction step, over 3 times excess amount of diol was used. The hydroxyl group of the alkyl chain-end was converted to a tosylate group because it is easily converted to an iodide group by substitution. Alkyl iodide is the most susceptible halide to Michaelis–Arbuzov reaction,[33] which is a widely used method to make carbon–phosphorus bonds. Normally, the primary alkyl halide can be transformed to an alkyl phosphonate at the temperature of 150 to 160 °C without any solvent or catalyst in the Michaelis-Arbuzov reaction. But in the phosphonation-step of these systems with vinyl group (preparation of **5a** and **5b**), the reaction temperature should be controlled below 125 °C. When the temperature was as high as 120–125 °C, a reaction mixture without hydroquinone gradually became viscous and finally yielded a gel-like product because of the polymerization of the vinyl groups. After purification by a silica-gel column chromatography, the yield of this phosphonation-step without hydroquinone was as low as 30%. To minimize the thermal polymerization, 0.03 mol % of hydroquinone was added as an inhibitor. As a result, the phosphonation reaction proceeded quite well at 120 °C with the yield of over 70%. Hydrolysis of the phosphonate group was accomplished under mild condition by using bromotrimethylsilane. Generally, phosphonate groups can be hydrolyzed to phosphonic acids in an aqueous solution of strong acids such as HCl, HBr under reflux. However, the vinyl group in the monomer can be saturated under such highly acidic conditions.[34] In addition, highly basic condition is not feasible either, because phosphonate cannot be fully hydrolyzed and monoester of phosphonic acid can be obtained.[35] Therefore, bromotrimethylsilane was used for mild hydrolysis to avoid undesirable side products, and the phosphonate compound was fully hydrolyzed to phosphonic acid at room temperature.[36,37]

All polymers were prepared by free radical polymerization of monomers **6a** and **6b** as shown in Scheme 2. Phosphonic acid monomers **6a** and **6b** were polymerized in mixture of 1,4-dioxane and deionized water with AIBA as a water-soluble initiator. The resulting polymers were purified by dialysis in deionized water medium using a separation-membrane with approximately a M_n = 2000 g/mol cutoff. PVBPA-Ethyl was quite soluble in water and the solution was transparent during dialysis. The solubility of PVBPA-Hexyl in water was not as good as indicated by the turbidity of the solution. The resulting polymers, after removal of water by freeze-drying, were

dx.doi.org/10.1021/cm202064x | Chem. Mater. 2012, 24, 115–122

yellowish-white solids. The molecular masses of polymers were analyzed by an aqueous GPC. The weight-averaged molecular masses of PVBPA-Ethyl and PVBPA-Hexyl were approximately 25 000 and 22 000 g/mol, respectively, with a relatively narrow polydispersity index of 1.4 for both samples. Molecular masses are relative values against PEG standard. Measuring the absolute molecular mass of PVBPA with GPC is a rather complicated problem, since the molecular mass per a skeletal bond of PVBPA monomer is much larger, by ca. 8 times, than PEG monomer, and the hydrodynamic volume of PVBPA is affected by the polyelectrolyte effects screened in part by the buffer.[20]

Thermal Stability. The thermal stability of the polymers was characterized by TGA under nitrogen at a heating rate of 10 °C/min. Figure 1a shows the temperature-dependent mass

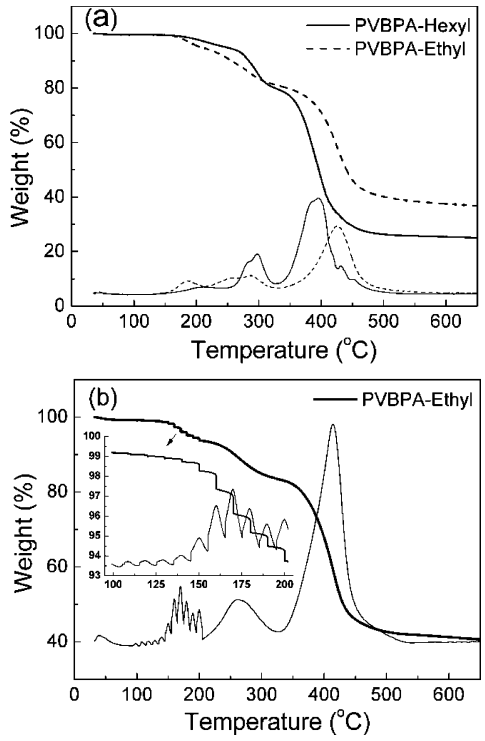

Figure 1. Thermal mass loss characteristics investigated by thermogravimetric analysis (TGA): (a) continuous heating at 10 °C/min and (b) step-isothermal heating for 5 min at each temperature of 10 °C interval from 100 to 200 °C. The bottom portion shows the temperature derivatives of mass loss and the inset is the expanded plot of the 100 to 200 °C region.

loss of these materials. In both samples, the first mass-loss process appears between 150 and 230 °C. This degradation is consistent with the loss of water by self-condensation of the phosphonic acid groups. The second mass-loss process occurs between 230 and 330 °C and is attributed to the removal of the side-chains attached to the polystyrene backbone by cleavage of ether bonds. The polymer backbone starts to decompose above 330 °C, resulting in further mass loss. Such a thermal degradation tendency is consistent with the previous result obtained from poly(vinylbenzylphosphonic acid).[31] To determine the onset temperature of self-condensation between phosphonic acid groups, step-isothermal TGA experiments were carried out between 100 and 200 °C, by increasing the temperature from 100 °C in intervals of 10 °C with a rate of 10 °C/min and then maintaining the temperature for 5 min at each step. This result is shown in Figure 1b for PVBPA-Ethyl, where the steps in the mass loss are seen in temperature-range between 100 and 200 °C. From 100 to 140 °C, the extent of the mass loss is small, but above 150 °C the amount of mass loss became quite significant. PVBPA-Hexyl also shows a similar response. Our interpretation of these step-isothermal TGA experiments is that these polymers are thermally stable up to 140 °C against the self-condensation of phosphonic acid groups.

Small-Angle X-ray Scattering Measurements. In order to ascertain the formation of proton-conducting channels in the PVBPA polymers, small-angle X-ray scattering experiments were performed at room temperature on solvent-cast and dried films. As shown in Figure 2, there are well-defined maxima in

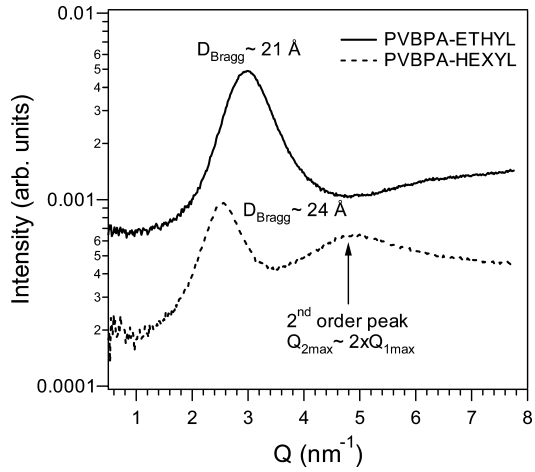

Figure 2. Small-angle X-ray scattering (SAXS) profile measured at room temperature. The Bragg spacing, ~(21 ± 1) Å, indicates that the side chains form a bilayer lamellar structure.

the scattering intensity for both PVBPA-Ethyl and PVBPA-Hexyl samples. The Q_{max} of these peaks correspond to a Bragg-spacing of approximately (21 ± 1) Å and (24 ± 1) Å for PVBPA-Ethyl and PVBPA-Hexyl, respectively. In addition, the PVBPA-Hexyl sample shows a second order peak at $Q_{2\text{-max}}$ that is approximately twice the value of the first peak $Q_{1\text{-max}}$. A rough estimate based on the molecular structure indicates that the distance between the phosphonic acid moiety and the polymer backbone for PVBPA-Ethyl is approximately 10 Å. This is about one-half the value of the Bragg spacing determined from the scattering maximum. These data are consistent with the notion that the phosphonic acid-containing side-chains, through aggregation of the acidic groups, form a bilayer or lamellar-like proton-conducting channel structure. It is not surprising considering that it is known that phosphonate-containing surfactants readily form a number of nanostructured micellar phases.[38,39] This bilayer structure is quite different from the proposed core-shell structure of Nafion.[32,40]

Thermal Relaxation Characteristic. DSC and DMA measurements were carried out to investigate the thermo-mechanical relaxation properties of these polymers, related to the bilayer-type nanostructure in bulk films. In the DSC thermograms shown in Figure 3a, the glass transition temperature (T_g) was determined from the midpoint of the step-change in the heat capacity. The T_gs for the different materials are very similar, $T_g \approx 20$ °C, with no apparent

dx.doi.org/10.1021/cm202064x | Chem. Mater. 2012, 24, 115–122

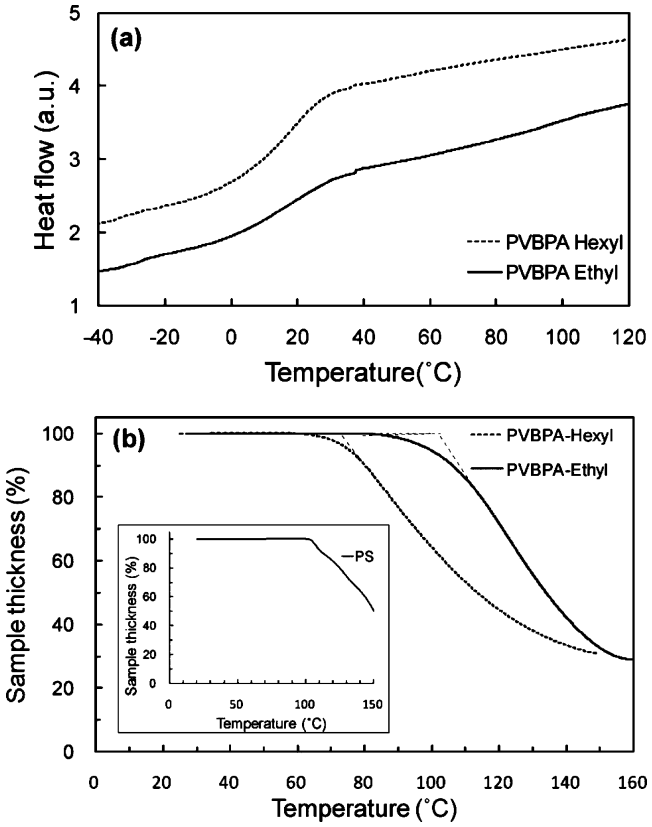

Figure 3. (a) Thermal analysis of PVBPA-Ethyl and PVBPA-Hexyl samples by DSC. (b) Thermal relaxation analysis by DMA penetration-method under 0.5 N load for PVBPA-Ethyl and PVBPA-Hexyl samples. The data for the reference sample of polystyrene with a known T_g of 100 °C are shown in the inset. The T_g value was determined at the intersect of two extension lines. The average error is approximately ±2 °C.

dependence on the side-chain length; the DSC T_gs of the two materials differ by less than a few degrees. However, the probe penetration measurements using the DMA instrument show a very interesting thermal softening response in the region above the DSC T_g as shown in Figure 3b. This particular technique may be slightly more sensitive to the molecular motions within the materials that do not give rise to detectable jump in the heat capacity by DSC due to a very broad transition. Since the DMA data start at 20 °C, essentially the midpoint of the DSC T_g, we cannot quantitatively compare the DSC T_g to the softening transition measured by DMA. However, there appears to be an additional, higher softening temperature, at $T \approx 101$ °C for the PVBPA-Ethyl and $T \approx 74$ °C for the PVBPA-Hexyl. Although only a single, similar T_g was observed for both samples by DSC, it is likely that the mechanical measurements are more sensitive to subtle differences in the molecular motions that give rise to bulk mechanical relaxations. It is not surprising that PVBPA-Hexyl would have a slightly lower temperature for softening than PVBPA-Ethyl because the increased flexibility of the hexyl group is likely to facilitate molecular motions at lower temperatures. The samples appear relatively glassy at room temperature, so the transition measured by DSC could be due to molecular motions within phosphonic acid aggregated channels or network as described for other ion-containing polymers. There does appear to be some softening of the material near the calorimetric T_g, but significant softening does not occur until much higher temperatures and is also dependent upon the side-chain length. This higher-temperature softening is likely due to the molecular relaxations in the polystyrene-like phase-separated domain.

Proton Conductivity Measurements. The conductivity measurements of both PVBPA-Ethyl and PVBPA-Hexyl were performed using broadband dielectric relaxation spectroscopy (DRS) under dry nitrogen gas flow. The results of the frequency dependent conductivity measurements are shown in Figure 4 as a function of frequency at various temperatures.

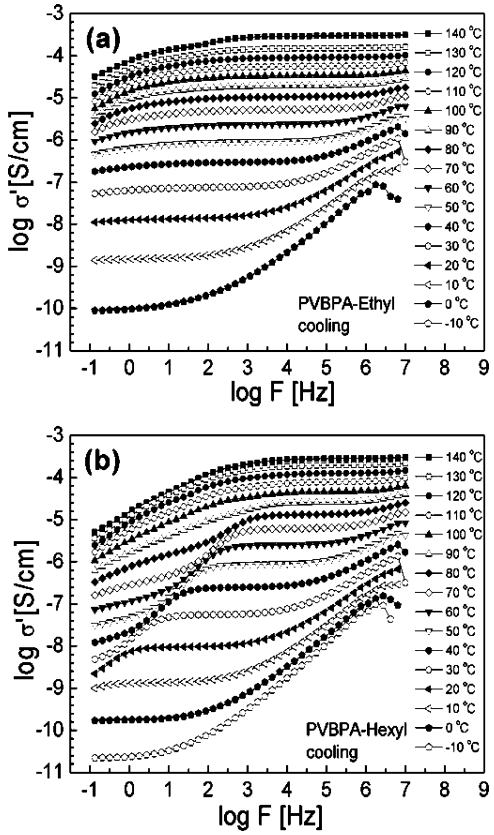

Figure 4. AC conductivity versus frequency of (a) PVBPA-Ethyl and (b) PVBPA-Hexyl at various temperatures. The standard error for the reported conductivity is on the order of 0.2% of the magnitude of the conductivity.

Each sample is characterized by a frequency independent (DC) conductivity plateau. These plateau regions develop at frequencies below the segmental relaxation, and move to higher frequencies as the segmental relaxation moves to higher frequencies. There is a sharp drop in the conductivity on the low frequency side of this plateau which is caused by electrode polarization. The temperature-dependent direct current (DC) conductivity of the samples was estimated from plateau values in the AC conductivity in a frequency scan at each temperature, ignoring the electrode polarization effects.[21,23,41] The DC conductivities are plotted as a function of inverse temperature in Figure 5. The data shown include both samples over a heating and cooling cycle. It appears that the two polymers containing different side-chains have similar conductivity behavior in the measured temperature regime. This may be due to the fact that the hexyl system has a lower volume fraction of acid groups, but forms a better organized acid aggregate structure for charge transport, consistent with the SAXS results in Figure 2.

dx.doi.org/10.1021/cm202064x | *Chem. Mater.* 2012, 24, 115–122

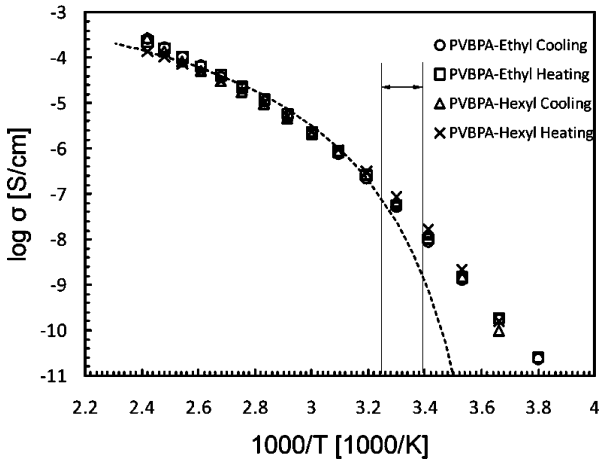

Figure 5. Temperature-dependent proton conductivity of the synthesized polymers determined by broadband dielectric relaxation spectroscopy. The line represents an average fit of the VFT equation to the data in the high-temperature range. The two vertical lines denote the T_g estimated from T_o and the calorimetric T_g, respectively.. The four plots for the two polymers during heating and cooling are hardly distinguishable and hence are treated as a single plot. The average error associated with each point is approximately ±10% of the magnitude of the measured conductivity, σ.

We have performed a semiquantitative fit to the data with Vogel–Fulcher–Tamman (VFT) equation:

$$\sigma = \sigma_o \exp\left[\frac{-B}{T - T_o}\right]$$

where σ_o is the conductivity at infinite temperature (4.75×10^{-3} S/cm), B is a constant with units of temperature (550K), and T_o is the temperature below which ion motion should cease (so-called Vogel–Fulcher temperature, usually ~50 °C below the normal glass transition temperature T_g[42,43]). From a qualitative perspective, the VFT equation does a reasonable job at parametrizing the data above the temperature range denoted by the two vertical lines in Figure 5. As the temperature drops below this region, the data follow an Arrhenius-type behavior. The agreement of the high temperature portion with the VFT equation indicates that the charge motion is coupled to the motions of the polymer segments. This is likely facilitated through a Grotthus hopping mechanism.[44−46] A fit of the VFT equation through all data can be forced, but the fitting parameters then become nonphysical and are no longer useful. From a more quantitative analysis, the T_g estimated from the T_o (258 K) was found to be approximately 35 °C (the vertical line on 3.25 [1000/K]), which is comparable to the T_g measured by DSC (20 °C, the vertical line on 3.41 [1000/K]). Moreover, the experimental data start to deviate from the VFT equation at the temperatures below these two vertical lines. In conclusion, it seems that the fitting parameters are consistent with the proton conduction taking place in the phosphonic acid aggregated channels, wherein significant segmental motions occur above the T_g indicated by the DSC data.

Finally, it is important to note that the proton conductivity of our samples under nominally dry conditions at 25 °C was found to be approximately 3×10^{-8} S/cm, which is much higher than the values from poly(vinylbenzylphosphonic acid) (1×10^{-10} to 1×10^{-11} S/cm).[30,31] The much higher proton conductivities in these polymers under nominally dry conditions may be attributed to the highly aggregated proton-conducting acid channels with mobile hydrogen bond network, as evidenced by the existence of the nanophase separated domains shown by SAXS results. It was previously reported in the case of immobilized imidazoles that longer alkyl chain tethered protogenic groups result in higher conductivity.[13,47,48] This phenomenon was explained by chain flexibility which enables less restriction for aggregation of protogenic group and hydrogen bond formation,[12,49] but no supporting structural evidence was provided. Similarly, Steininger et al.[50] investigated cyclic siloxanes with tethered phosphonic acid groups via flexible spacers, but no structural information on aggregation or nanophase separation was shown.

CONCLUSIONS

In this paper we have reported the synthesis and characterization of phosphonic acid functionalized polystyrene derivatives. Poly(vinylbenzyloxy-alkyl-phosphonic acid)s with two different alkyl side chains (ethyl and hexyl) are successfully synthesized by Michaelis–Arbuzov and other synthetic methods. The synthesized polymers exhibit a narrow polydispersity index of about 1.4 and molecular masses of approximately $M_w \approx 24\,000$ g/mol by aqueous gel permeation chromatography (GPC) with PEG standards and thermal stability up to 140 °C. The phosphonic acid groups undergo condensation with the loss of water above 140 °C. Both polymers show nanophase-separated morphology with characteristic domain spacing of ca. 2 nm, which is attributed to a bilayer lamellar-type organization of the surfactant-like side chains. The proton conductivities are found to be approximately 2.6×10^{-4} S/cm at 140 °C under nominally anhydrous condition by broadband dielectric relaxation spectroscopy. The proton transport may occur through Grotthuss mechanism (structure diffusion) which consists of aggregated protogenic charge carriers and dynamic hydrogen bond formation. Further optimized nanophase-separation morphology and molecular dynamics of percolated phosphonic-acid channels would lead to improved polymer electrolyte membranes for anhydrous fuel cells with higher proton conductivity and better mechanical properties.

ASSOCIATED CONTENT

Supporting Information

^{1}H NMR and ^{13}C NMR spectra of all the synthesized compounds. This material is available free of charge via the Internet at http://pubs.acs.org

AUTHOR INFORMATION

Corresponding Author

*E-mail: dyyoon@snu.ac.kr (D.Y.Y.); kirt.page@nist.gov (K.A.P.).

ACKNOWLEDGMENTS

We thank Dr. W. Meyer and Prof. G. Wegner for helpful discussions and advice. This work was supported by the Chemistry and Molecular Engineering Program of the Brain Korea 21 Project, LG Chem., Ltd., and National Research Foundation of Korea (R01-2008-000-11971-0).

REFERENCES

(1) Barbir, F. *PEM Fuel Cells: Theory and Practice*; Elsevier: London, 2005.

(2) Winter, M.; Brodd, R. J. *Chem. Rev.* **2004**, *104*, 4245.
(3) Zawodzinski, J. T. A.; Derouin, C.; Radzinski, S.; Sherman, R. J.; Smith, V. T.; Springer, T. E.; Gottesfeld, S. *J. Electrochem. Soc.* **1993**, *140*, 1041.
(4) Basu, S. *Recent Trends in Fuel Cell Science and Technology*; Springer: New York, 2007.
(5) Smitha, B.; Sridhar, S.; Khan, A. A. *J. Membr. Sci.* **2005**, *259*, 10.
(6) Kreuer, K. D. *J. Membr. Sci.* **2001**, *185*, 29.
(7) Gubler, L.; Scherer, G. G. *Desalination* **2010**, *250*, 1034.
(8) Schuster, M. F. H.; Meyer, W. H. *Annu. Rev. Mater. Res.* **2003**, *33*, 233.
(9) Kreuer, K.-D.; Paddison, S. J.; Spohr, E.; Schuster, M. *Chem. Rev.* **2004**, *104*, 4637.
(10) Steininger, H.; Schuster, M.; Kreuer, K. D.; Kaltbeitzel, A.; Bingol, B.; Meyer, W. H.; Schauff, S.; Brunklaus, G.; Maier, J.; Spiess, H. W. *Phys. Chem. Chem. Phys.* **2007**, *9*, 1764.
(11) Wainright, J. S.; Wang, J. T.; Weng, D.; Savinell, R. F.; Litt, M. *J. Electrochem. Soc.* **1995**, *142*, L121.
(12) Kerres, J. A. *J. Membr. Sci.* **2001**, *185*, 3.
(13) Schuster, M. F. H.; Meyer, W. H.; Schuster, M.; Kreuer, K. D. *Chem. Mater.* **2004**, *16*, 329.
(14) Persson, J. C.; Jannasch, P. *Macromolecules* **2005**, *38*, 3283.
(15) Kreuer, K. D.; Fuchs, A.; Ise, M.; Spaeth, M.; Maier, J. *Electrochim. Acta* **1998**, *43*, 1281.
(16) Herz, H. G.; Kreuer, K. D.; Maier, J.; Scharfenberger, G.; Schuster, M. F. H.; Meyer, W. H. *Electrochim. Acta* **2003**, *48*, 2165.
(17) de Grotthuss, C. J. T. *Ann. Chim.* **1806**, *58*, 54.
(18) Agmon, N. *Chem. Phys. Lett.* **1995**, *244*, 456.
(19) Schuster, M.; Rager, T.; Noda, A.; Kreuer, K. D.; Maier, J. *Fuel Cells* **2005**, *5*, 355.
(20) Bingol, B.; Meyer, W. H.; Wagner, M.; Wegner, G. *Macromol. Rapid Commun.* **2006**, *27*, 1719.
(21) Bozkurt, A.; Meyer, W. H.; Gutmann, J.; Wegner, G. *Solid State Ionics* **2003**, *164*, 169.
(22) Erdemi, H.; Bozkurt, A. *Eur. Polym. J.* **2004**, *40*, 1925.
(23) Sevil, F.; Bozkurt, A. *J. Phys. Chem. Solids* **2004**, *65*, 1659.
(24) Yamada, M.; Honma, I. *Polymer* **2005**, *46*, 2986.
(25) Yamada, M.; Honma, I. *Angew. Chem., Int. Ed.* **2004**, *43*, 3688.
(26) Yamada, M.; Honma, I. *J. Phys. Chem. B* **2004**, *108*, 5522.
(27) Rager, T.; Schuster, M.; Steininger, H.; Kreuer, K.-D. *Adv. Mater.* **2007**, *19*, 3317.
(28) Parvole, J.; Jannasch, P. *Macromolecules* **2008**, *41*, 3893.
(29) Rusanov, A. L.; Kostoglodov, P. V.; Abadie, M. J. M.; Voytekunas, V. Y.; Likhachev, D. Y. *Fuel Cells II*; Springer-Verlag: Berlin, 2008; Vol. *216*, p 125.
(30) Jiang, F.; Kaltbeitzel, A.; Meyer, W. H.; Pu, H.; Wegner, G. *Macromolecules* **2008**, *41*, 3081.
(31) Jiang, F.; Kaltbeitzel, A.; Fassbender, B.; Brunklaus, G.; Pu, H.; Meyer, W. H.; Spiess, H. W.; Wegner, G. *Macromol. Chem. Phys.* **2008**, *209*, 2494.
(32) Schmidt-Rohr, K.; Chen, Q. *Nat. Mater.* **2008**, *7*, 75.
(33) Bhattacharya, A. K.; Thyagarajan, G. *Chem. Rev.* **1981**, *81*, 415.
(34) Boutevin, B.; Hamoui, B.; Parisi, J.-P.; Améduri, B. *Eur. Polym. J.* **1996**, *32*, 159.
(35) Rabinowitz, R. *J. Am. Chem. Soc.* **1960**, *82*, 4564.
(36) Rabinowitz, R. *J. Org. Chem.* **1963**, *28*, 2975.
(37) Souzy, R.; Ameduri, B.; Boutevin, B.; Virieux, D. *J. Fluorine Chem.* **2004**, *125*, 1317.
(38) Ma, T.-Y.; Zhang, X.-J.; Yuan, Z.-Y. *J. Phys. Chem. C* **2009**, *113*, 12854−12862.
(39) Malone, S. M.; Trabelsi, S.; Zhang, S.; Lee, T. R.; Schwartz, D. K. *J. Phys. Chem. B* **2010**, *114*, 8616−8620.
(40) Haubold, H.-G.; Vad, Th.; Hiller, H. J. P. *Electrochim. Acta* **2001**, *46*, 1559.
(41) Bozkurt, A.; Ise, M.; Kreuer, K. D.; Meyer, W. H.; Wegner, G. *Solid State Ionics* **1999**, *125*, 225.
(42) Schoenhals, A.; Kremer, F.; Hofmann, A.; Fischer, E. W.; Schlosser, E. *Phys. Rev. Lett.* **1993**, *70*, 3459.
(43) Ratner, M. A.; Nitzan, A. *Faraday Discuss. Chem. Soc.* **1989**, *88*, 19.
(44) Steinkam, K.; Schumacher, J. O.; Goldsmith, F.; Ohlberger, M.; Ziegler, C. *J. Fuel Cell Sci. Technol.* **2008**, *5*, 011007−1−16.
(45) Lott, K. F.; Ghosh, B. D.; Ritchie, J. E. *J. Electrochem. Soc.* **2006**, *153*, A2044−A2048.
(46) Lott, K. F.; Ghosh, B. D.; Ritchie, J. E. *Electrochem. Solid-State Lett.* **2005**, *8*, A513−A515.
(47) Schuster, M.; Meyer, W. H.; Wegner, G.; Herz, H. G.; Ise, M.; Kreuer, K. D.; Maier, J. *Solid State Ionics* **2001**, *145*, 85.
(48) Persson, J. C.; Jannasch, P. *Chem. Mater.* **2003**, *15*, 3044.
(49) Kreuer, K.-D. *Chem. Phys. Chem.* **2002**, *3*, 771.
(50) Steininger, H.; Schuster, M.; Kreuer, K. D.; Maier, J. *Solid State Ionics* **2006**, *177*, 2457.